Orbital Hall effect accompanying the quantum Hall effect: Landau levels cause orbital polarized edge currents
— Supplemental Material —

Börge Göbel* and Ingrid Mertig

Institut für Physik, Martin-Luther-Universität

Halle-Wittenberg, D-06099 Halle (Saale), Germany

1. METHODS: TIGHT-BINDING MODEL

We consider one s orbital per lattice site. The spin is disregarded in our calculations as it plays no essential role for the quantum and orbital Hall effects. We restrict the hopping terms to nearest neighbors. The two-dimensional system is defined by the lattice vectors $\boldsymbol{a}_1 = a\boldsymbol{e}_x$ and $\boldsymbol{a}_2 = a\boldsymbol{e}_y$ with the lattice constant a. Without a magnetic field, the band structure is $E(\boldsymbol{k}) = 2t\,[\cos(k_x a) + \cos(k_y a)]$.

With magnetic field, the Hamiltonian can be represented by the matrix

$$H = t_0 \begin{pmatrix} h_1 & \mathrm{e}^{iak_y} & 0 & \dots & 0 & c\mathrm{e}^{-iak_y} \\ \mathrm{e}^{-iak_y} & h_2 & e^{iak_y} & \dots & 0 & 0 \\ 0 & \mathrm{e}^{-iak_y} & h_3 & \dots & 0 & 0 \\ \vdots & \vdots & \vdots & \ddots & \vdots & \vdots \\ 0 & 0 & 0 & \dots & h_{q_0-1} & \mathrm{e}^{iak_y} \\ c\mathrm{e}^{iak_y} & 0 & 0 & \dots & \mathrm{e}^{-iak_y} & h_{q_0} \end{pmatrix},$$

with $t_0 = -1\,\mathrm{eV}$. q_0 is the number of atoms in the unit cell and $c = 0$ or 1 controls the periodic boundary conditions along y. The diagonal terms are

$$h_j = 2\cos\left(ak_x - 2\pi\frac{p}{q}j\right).$$

Note that while $B = \frac{1}{a^2}\frac{h}{e}\frac{p}{q}$ is in general a real number, any value can be approximated to any desired precision by a rational number $\frac{p}{q}$. To simulate a bulk sample (periodic along x and y, as in Fig. 2) we set $c = 1$ and $q_0 = q$. To simulate a slab (as in Fig. 1) which is only periodic along the x direction, we set $c = 0$. Diagonalization of the Hamiltonian gives rise to the band structure $E_{\nu\boldsymbol{k}}$ and the eigenvectors $|\nu\boldsymbol{k}\rangle$.

2. METHODS: CALCULATION OF THE OBSERVABLES

The intrinsic quantum Hall conductivity [1]

$$\sigma_{xy}(E_\mathrm{F}) = -\frac{e^2}{h} \sum_\nu \frac{1}{2\pi} \int_{E_{\nu\boldsymbol{k}} \leq E_\mathrm{F}} \Omega_{\nu,z}(\boldsymbol{k})\, \mathrm{d}^2 k. \tag{1}$$

is calculated from the reciprocal space Berry curvature [2]

$$\Omega_{\nu,z}(\boldsymbol{k}) = -2\hbar^2\ \mathrm{Im} \sum_{\mu\neq\nu} \frac{\langle \nu\boldsymbol{k}|v_x|\mu\boldsymbol{k}\rangle\langle \mu\boldsymbol{k}|v_y|\nu\boldsymbol{k}\rangle}{(E_{\nu\boldsymbol{k}} - E_{\mu\boldsymbol{k}})^2} \tag{2}$$

as a Brillouin zone integral over all occupied states (states below the Fermi energy E_F at zero temperature).

The orbital Hall conductivity [3]

$$\sigma_{xy}^{L_z}(E_\mathrm{F}) = \frac{e}{\hbar} \sum_\nu \frac{1}{(2\pi)^2} \int_{E_{\nu\boldsymbol{k}} \leq E_\mathrm{F}} \Omega_{\nu,z}^{L_z}(\boldsymbol{k})\, \mathrm{d}^2 k. \tag{3}$$

is calculated from the orbital Berry curvature

$$\Omega_{\nu,z}^{L_z}(\boldsymbol{k}) = -2\hbar^2\ \mathrm{Im} \sum_{\mu\neq\nu} \frac{\langle \nu\boldsymbol{k}|j_x^z|\mu\boldsymbol{k}\rangle\langle \mu\boldsymbol{k}|v_y|\nu\boldsymbol{k}\rangle}{(E_{\nu\boldsymbol{k}} - E_{\mu\boldsymbol{k}})^2}. \tag{4}$$

with the orbital current operator

$$\langle \nu\boldsymbol{k}|j_x^z|\mu\boldsymbol{k}\rangle = \frac{1}{2}\sum_\alpha [\langle \nu\boldsymbol{k}|v_x|\alpha\boldsymbol{k}\rangle\langle \alpha\boldsymbol{k}|L_z|\mu\boldsymbol{k}\rangle + \langle \nu\boldsymbol{k}|L_z|\alpha\boldsymbol{k}\rangle\langle \alpha\boldsymbol{k}|v_x|\mu\boldsymbol{k}\rangle]. \tag{5}$$

The orbital magnetization is calculated based on the modern formulation [4–9]

$$M_z(E_\mathrm{F}) = \frac{-1}{(2\pi)^2} \sum_\nu \left[\frac{g_L \mu_B}{\hbar} \int_{E_{\mu\boldsymbol{k}} \leq E_\mathrm{F}} L_{\nu,z}(\boldsymbol{k})\, \mathrm{d}^2 k - \frac{e}{\hbar} \int_{E_{\mu\boldsymbol{k}} \leq E_\mathrm{F}} \Omega_{\nu,z}(\boldsymbol{k}) \cdot [E_\mathrm{F} - E_{\mu\boldsymbol{k}}]\, \mathrm{d}^2 k \right] \tag{6}$$

as the integral over the diagonal elements of the orbital angular momentum

$$m_\nu^z(\boldsymbol{k}) = -L_{\nu\nu}^z(\boldsymbol{k}) \cdot \frac{g_L \mu_B}{\hbar} = -i\frac{e\hbar}{2} \sum_{\beta\neq\nu} \frac{\langle \nu\boldsymbol{k}|v_x|\beta\boldsymbol{k}\rangle\langle \beta\boldsymbol{k}|v_y|\alpha\boldsymbol{k}\rangle - \langle \nu\boldsymbol{k}|v_y|\beta\boldsymbol{k}\rangle\langle \beta\boldsymbol{k}|v_x|\alpha\boldsymbol{k}\rangle}{E_{\beta\boldsymbol{k}} - E_{\nu\boldsymbol{k}}} \tag{7}$$

plus a correction term that occurs due to the emergence of a reciprocal space Berry curvature [5].

3. DISCUSSION OF THE QUANTIZATION

Even though the quantum Hall system investigated in this paper is in a topological phase and the Landau levels have finite Chern numbers

$$C_\nu = \int \Omega_{\nu,z}(\boldsymbol{k})\,\mathrm{d}^2k, \tag{8}$$

causing chiral edge states, the values of the orbital Hall resistivity plateaus are not quantized. This is because the orbital angular momentum is not a good quantum number and can, in principle, be arbitrarily large. This is reminiscent of a $\mathbb{Z}_2$ topological insulator with Rashba-interaction for which the spin is not a good quantum number and the spin Hall conductivity is not quantized in the gap, even though the spin Chern number is integer [10–15]. Recently, progress has been made in the development of the theory of orbital Chern numbers but there is still a lack of formal equivalence with a topological invariant [15, 16].

4. MEASUREMENT OF ORBITAL CURRENTS

The measurement of orbital currents is an actively discussed field at the moment and we follow a review [17] to clarify this issue. A lack of direct measurement methods calls for additional explanations on how the orbital currents can be measured in an experiment. To measure signatures of orbital currents, three main approaches have been considered in the literature: (a) Detection via orbital torque, (b) detection of the accumulation, and (c) detection via inverse effects.

(a) Orbital currents can be detected via orbital torque. Here, the orbital current is injected into a ferromagnet that is attached to the system under investigation. Indeed, the transported orbital angular momentum does not directly interact with the spin magnetization of the ferromagnet. However, the spin-orbit coupling in the ferromagnet transforms the orbital current into a spin current that induces a torque. Since the spin-orbit coupling of the ferromagnet is known in the experiment, the orbital current can be determined. This is the technique that was used in several publications to measure orbital currents like Ref. [18]. It is feasible also in our scenario as charge currents do not generate torques.

(b) Another method is to measure the accumulation at the edge of the sample. The advantage of this method is that no additional layer is needed for the experiment. Since orbital currents lead to accumulation at the edges, there is a finite orbital angular momentum. A Kerr rotation of reflected light can be measured via the magneto-optical Kerr effect (MOKE). This method has been used for example in Ref. [19] and Ref. [20]. It might be particularly interesting in our scenario: The orbital currents emerge as edge states, so it might be possible to resolve them directly by this method. Besides the MOKE, the orbital Hanle magnetoresistance has been used to measure orbital currents according to Ref. [21].

(c) Orbital signatures can also be measured by inverse effects as has been done for the orbital Edelstein effect in Ref. [22]. Orbital pumping from an attached ferromagnet introduces orbital currents into the system under investigation. According to Onsager's relation, an inverse orbital Hall effect exists when the sample exhibits an orbital Hall effect. This inverse effect translates the orbital current into a charge current, that can be measured. In our case, this might cause a problem because we do not have a pure orbital Hall effect but a (charge) Hall effect as well. Still the calculated characteristic dependence on the magnetic field (quadratic vs. linear) will allow to distinguish the two contributions.

5. RESULTS: VARIATION OF THE MAGNETIC FIELD

Fig. S1 shows results similar to Fig. 2 of the main text but for $p = 1$ and $q = 17$.

Fig. S2 corresponds to $p = 3$ and $q = 52$. The results can easily be related to the case $p/q = 1/17$, as presented in Fig. S1 because $\frac{p}{q} = \frac{3}{52} = \frac{1}{17+\frac{1}{3}}$. The Landau levels in (a) form bundles of three, except for the one near $E = 0$ where a bundle of 4 is formed. The total Chern number of the Landau level bundles is the same as for the case $p/q = 1/17$ but the Chern numbers of individual Landau levels can be much larger causing the spikes in σ_{xy} and especially $\sigma_{xy}^{L_z}$ in (b) and (c) respectively. However, due to the small energy difference between the Landau levels of one bundle, these spikes do not survive at finite temperatures.

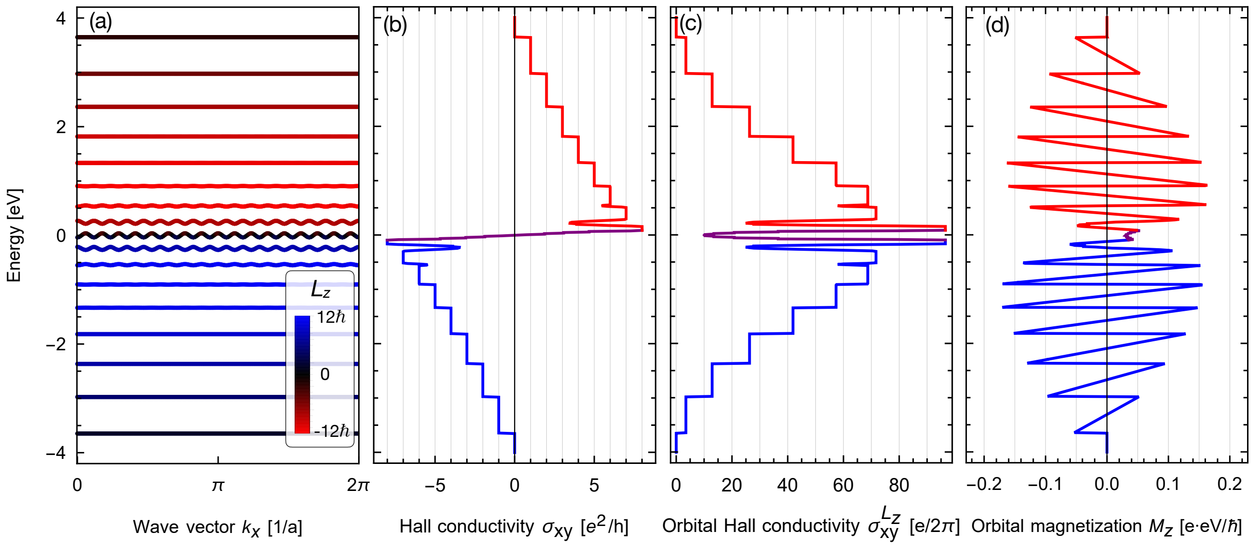

Figure S1. Tight-binding calculations for $p/q = 1/17$. (a) Band structure under strong magnetic field. Landau levels emerge and carry orbital angular momentum L_z (blue: positive, red: negative). (b) Charge Hall conductivity that is quantized in units of e^2/h in the band gaps. (c) Orbital Hall conductivity that is constant in the band gaps. (d) Orbital magnetization M_z.

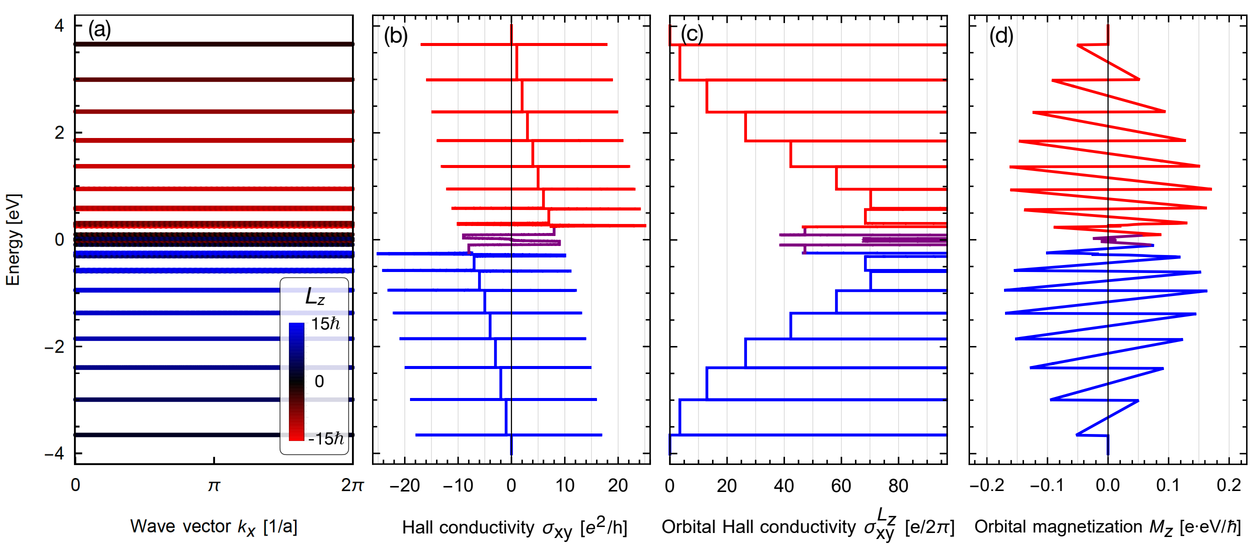

Figure S2. Tight-binding calculations for $p/q = 3/52$. (a) Band structure under strong magnetic field. Landau levels emerge and carry orbital angular momentum L_z (blue: positive, red: negative). (b) Charge Hall conductivity that is quantized in units of e^2/h in the band gaps. (c) Orbital Hall conductivity that is constant in the band gaps. (d) Orbital magnetization M_z.

6. RESULTS: DISORDER

The results presented in the main text rely on an intrinsic mechanism but have to survive also in dirty samples to be relevant. Fig. S3 shows results similar to Fig. S1 but for a dirty sample. Onsite energies have been varied randomly in the range of $[-0.2\,\mathrm{eV}, 0.2\,\mathrm{eV}]$. While the Landau levels deform in panel (a), the Hall conductivity (b), orbital Hall conductivity (c) and orbital magnetization (d) remain mostly the same and especially the plateaus in the Hall conductivities survive the disorder. The randomly generated onsite energies are:

$$
\begin{aligned}
&0.00557734\,\mathrm{eV}, 0.10926602\,\mathrm{eV}, 0.14817107\,\mathrm{eV}, -0.19678122\,\mathrm{eV}, -0.07610563\,\mathrm{eV},\\
&0.1830415\,\mathrm{eV}, 0.00524668\,\mathrm{eV}, -0.07268623\,\mathrm{eV}, 0.01567997\,\mathrm{eV}, -0.11149802\,\mathrm{eV},\\
&0.12259254\,\mathrm{eV}, -0.06309815\,\mathrm{eV}, 0.01555554\,\mathrm{eV}, -0.19765049\,\mathrm{eV}, 0.06926099\,\mathrm{eV},\\
&-0.1159903\,\mathrm{eV}, 0.17302304\,\mathrm{eV}.
\end{aligned}
$$

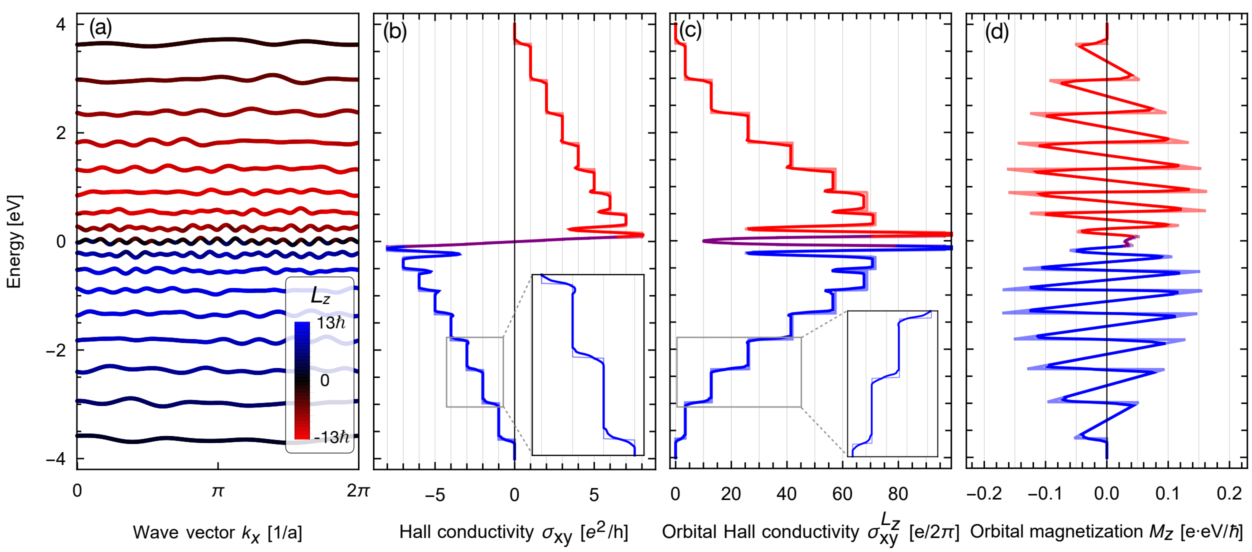

Figure S3. Tight-binding calculations for $p/q = 1/17$ in a dirty sample with randomly varying onsite energies in the range of $[-0.2\,\mathrm{eV}, 0.2\,\mathrm{eV}]$. (a) Band structure under strong magnetic field. Landau levels emerge and carry orbital angular momentum L_z (blue: positive, red: negative). (b) Charge Hall conductivity that is quantized in units of e^2/h in the band gaps. (c) Orbital Hall conductivity that is constant in the band gaps. (d) Orbital magnetization M_z. The bright curves in the background of panels (b-d) show the results of the clean sample.

7. RESULTS: TRIANGULAR LATTICE

To confirm that the results presented in the main text are fundamentally true, we have repeated the calculations on a triangular lattice [cf. Fig. S4]. Again, the results can be related to the zero-field band structure shown in panel (a) that is solely determined by the structural lattice. The main difference compared to the square lattice is that the Fermi line has two pockets in the energy range between 2 eV and 3 eV. Therefore, in this energy range the emerging Landau levels bundle in pairs of 2 and the Hall conductivity is quantized in units of $2e^2/h$. The sign change is again related to the location of the van Hove singularity which is at 2 eV for the triangular lattice. The main result discussed in the main text is the same: The quantum Hall effect is accompanied by an orbital Hall effect. Edge currents emerge that carry charge and orbital angular momentum.

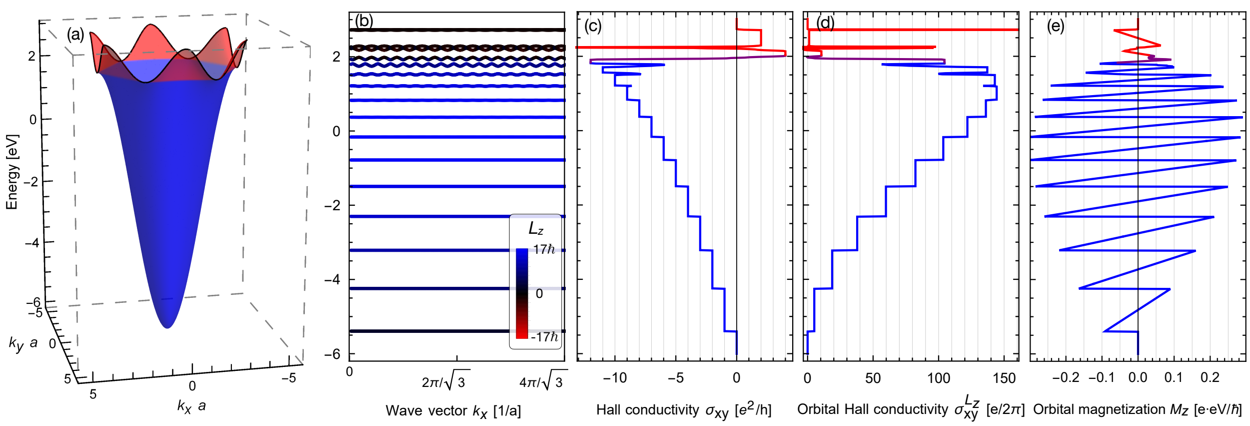

Figure S4. Tight-binding calculations for $p/q = 1/17$ on a triangular lattice. (a) Zero-field band structure of the triangular lattice. The color indicates the effective mass of the charge carriers (blue: electron-like, red: hole-like). (b) Band structure under strong magnetic field. Landau levels emerge and carry orbital angular momentum L_z (blue: positive, red: negative). (c) Charge Hall conductivity that is quantized in units of e^2/h in the band gaps. (d) Orbital Hall conductivity that is constant in the band gaps. (e) Orbital magnetization M_z.

---

* Correspondence email address: boerge.goebel@physik.uni-halle.de

[1] N. Nagaosa, J. Sinova, S. Onoda, A. H. MacDonald, and N. P. Ong, Rev. Mod. Phys. **82**, 1539 (2010).

[2] M. V. Berry, Proceedings of the Royal Society of London A: Mathematical, Physical and Engineering Sciences **392**, 45 (1984).

[3] A. Pezo, D. G. Ovalle, and A. Manchon, Phys. Rev. B **106**, 104414 (2022).

[4] M.-C. Chang and Q. Niu, Phys. Rev. B **53**, 7010 (1996).

[5] D. Xiao, J. Shi, and Q. Niu, Phys. Rev. Lett. **95**, 137204 (2005).

[6] T. Thonhauser, D. Ceresoli, D. Vanderbilt, and R. Resta, Phys. Rev. Lett. **95**, 137205 (2005).

[7] D. Ceresoli, T. Thonhauser, D. Vanderbilt, and R. Resta, Phys. Rev. B **74**, 024408 (2006).

[8] A. Raoux, F. Piéchon, J.-N. Fuchs, and G. Montambaux, Phys. Rev. B **91**, 085120 (2015).

[9] B. Göbel, A. Mook, J. Henk, and I. Mertig, Phys. Rev. B **99**, 060406 (2019).

[10] C. L. Kane and E. J. Mele, Phys. Rev. Lett. **95**, 226801 (2005).

[11] M. Ezawa, Phys. Rev. B **88**, 161406 (2013).

[12] E. Prodan, Phys. Rev. B **80**, 125327 (2009).

[13] Y. Yang, Z. Xu, L. Sheng, B. Wang, D. Xing, and D. Sheng, Phys. Rev. Lett. **107**, 066602 (2011).

[14] H. Li, L. Sheng, D. Sheng, and D. Xing, Phys. Rev. B **82**, 165104 (2010).

[15] T. P. Cysne, M. Costa, L. M. Canonico, M. B. Nardelli, R. Muniz, and T. G. Rappoport, Phys. Rev. Lett. **126**, 056601 (2021).

[16] A. L. Barbosa, L. M. Canonico, J. H. García, and T. G. Rappoport, Phys. Rev. B **110**, 085412 (2024).

[17] D. Jo, D. Go, G.-M. Choi, and H.-W. Lee, npj Spintronics **2**, 19 (2024).

[18] D. Lee, D. Go, H.-J. Park, W. Jeong, H.-W. Ko, D. Yun, D. Jo, S. Lee, G. Go, J. H. Oh, *et al.*, Nature Comms. **12**, 6710 (2021).

[19] Y.-G. Choi, D. Jo, K.-H. Ko, D. Go, K.-H. Kim, H. G. Park, C. Kim, B.-C. Min, G.-M. Choi, and H.-W. Lee, Nature **619**, 52 (2023).

[20] I. Lyalin, S. Alikhah, M. Berritta, P. M. Oppeneer, and R. K. Kawakami, Phys. Rev. Lett. **131**, 156702 (2023).

[21] G. Sala, H. Wang, W. Legrand, and P. Gambardella, Phys. Rev. Lett. **131**, 156703 (2023).

[22] A. El Hamdi, J.-Y. Chauleau, M. Boselli, C. Thibault, C. Gorini, A. Smogunov, C. Barreteau, S. Gariglio, J.-M. Triscone, and M. Viret, Nature Phys. **19**, 1855 (2023).